Dielectric relaxation spectroscopy and the ground state of $K_{1-x}Li_xTaO_3$

1989 J. Phys.: Condens. Matter 1 2241

(http://iopscience.iop.org/0953-8984/1/12/009)

J. Phys.: Condens. Matter 1 (1989) 2241–2256. Printed in the UK

Dielectric relaxation spectroscopy and the ground state of $K_{1-x}Li_xTaO_3$

U T Höchli and M Maglione†
IBM Research Division, Zurich Research Laboratory, 8803 Rüschlikon, Switzerland

Received 6 June 1988

Abstract. Dielectric susceptibility data are presented for frequencies between 10 and 10^9 Hz and for several Li concentrations. A low-frequency relaxation peak is attributed to an impurity mode slowing down to below 1 Hz at a concentration-dependent temperature. For Li concentrations $x \leqslant 0.04$, temperature-dependent relaxation rates and the broadening of relaxation peaks are accounted for by analytical and numerical predictions from spin-glass models. A high-frequency relaxation peak is attributed to the ordered motion of the lattice. Its relaxation rate increases with Li concentration. The lattice does not order ferroelectrically for any sample reported. The impurity modes for $x \geqslant 0.06$ exhibit disorder features that cannot be attributed to glass models nor to ferroelectricity. Non-random occupation of lattice sites by impurities could be at the origin of these features.

1. Introduction

$K_{1-x}Li_xTaO_3$ is a prototype of a system in which local dipoles occupy lattice sites at random. The local dipoles are attributed to Li ions which occupy K sites. They owe their dipole moment to their ionic size misfit which renders the centrosymmetric potassium site unstable. Figure 1 shows the structural misfit to scale. In the (1 0 0) plane occupied by oxygen and potassium ions, Li has four stable positions. Together with the two displacements perpendicular to the (1 0 0) plane, this amounts to association of Li to a dipole moment at the K site with six possible orientations.

These dipoles interact with one another and also polarise the lattice locally. Where this interaction is most important, namely at short distances, it is more complex than standard dipolar interaction. In view of their complexity and randomness, it is plausible to assume that certain pairs of dipoles tend to align parallel, others antiparallel or at 90°. For this case, Toulouse (1980) has shown that two parameters are relevant, namely the average interaction $\bar{J}_{ij}$, where i and j denote interacting pairs, and its standard deviation $\mathrm{Var}(J_{ij})$. He then predicted that the $T = 0$ ground state was non-trivially degenerate for all combinations of $\bar{J}$ and $\mathrm{Var}(J)$, except $\mathrm{Var}(J) = 0$, and that the ground state carried a moment exactly if $\bar{J} > \mathrm{Var}(J)$. We reproduce his findings in a diagram (figure 2) where we hatch the region of non-trivial degeneracy.

† Permanent address: Laboratoire de Physique du Solide, Université de Bourgogne, BP 138, F-21004 Dijon, France.

0953-8984/89/122241 + 16 $02.50

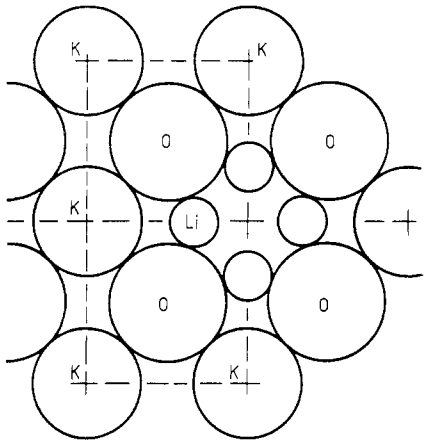

Figure 1. Cut [1 0 0] plane of perovskite $KTaO_3$. Note displacement of small-size Li. Drawing of ionic radii and structure to scale; K–K distance 4 Å. Of the four equivalent off-centre positions shown (plus two out of plane, not shown), only one is occupied by Li.

By studying the dynamical dipolar response as far into the hatched region as experimentally possible, we wish to characterise that ground state; in the language of phase transitions, this amounts to a study of precursor order.

Non-trivial degeneracy in Toulouse's (1980) sense implies a multitude of metastable states cascading in the direction of the ground state without ever reaching it. It also implies breakdown of periodic symmetry or, synonymously, cluster formation. While the cascading phenomenon entails slow dynamics, on which we shall dwell in this paper, cluster formation, or finite polar correlation, requires spatial resolution and detection of static polarisation. In the presence of metastability, the study of static polarisation and its spatial correlation may require enormous waiting times. We shall quote and discuss such investigations in the interpretation section and limit our investigation here to dynamics. The price to be paid for avoiding delays in the metastable range is the collection of a large number of data in a wide frequency, temperature and concentration range. This is what we shall pursue in the next section.

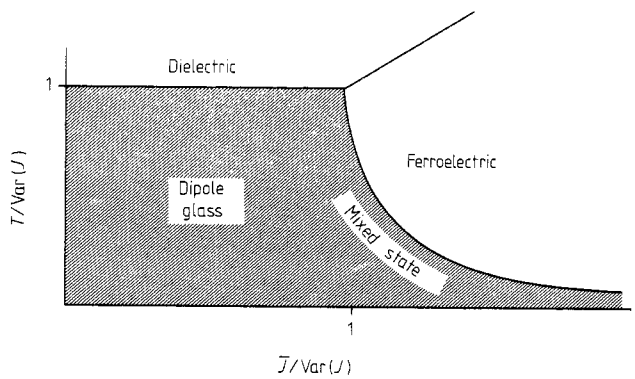

Figure 2. Phase diagram of random-interaction polar system (after Toulouse 1980). $\bar{J}$ average interaction, Var(J) standard deviation, T temperature. Hatched region: state with non-trivial degeneracy, mixed state has non-zero polarisation. Transitions experimentally accessible are dielectric to glass, dielectric to ferroelectric to mixed state.

2. Experiment

2.1. Method of dielectric spectroscopy

Generally speaking, the dielectric method provides information on long-wavelength polar motion in solids (see e.g. Jonscher 1983). It may also reveal evidence for inhomogeneity of the susceptibility in the sample, but does not provide spatial resolution (Bergmann 1978). To compare our data with model predictions, we must thus focus our attention on theoretical investigations on dynamical behaviour of disordered solids. They predict quite generally that the spectral density of motion extends to much wider frequency ranges than corresponding motion in ordered solids. This notion conditions our experimental search: first, we want to use as wide a frequency range as possible; secondly, we attempt to express the spectral density function in closed form for the sake of direct comparison of experimental with model parameters.

The extension of the experimental frequency range for dielectric spectroscopy to $10\ \text{Hz} \leqslant f \leqslant 10^9\ \text{Hz}$ required the installation of a vector wave-meter (hp 4191) operating with a remote sample (Maglione 1987). This implies use of different-shaped samples at different frequencies. To save the original samples used in earlier investigations (Van der Klink *et al* 1983), new samples were cut from the original ingots grown at the EPF, Lausanne, by Rytz (1984). Their dimensions were typically $1 \times 1 \times 1.5\ \text{mm}^3$, but sometimes up to three samples of varying dimensions had to be cut to avoid cavity resonances in the hp 4191 sample holder.

The report of ε^* at 10 temperatures, six concentrations and 80 frequencies comprises 9600 data points.

2.2. Experimental results

We start by presenting a typical dielectric spectrum $\varepsilon^*(\log \omega)$ for $K_{1-x}Li_xTaO_3$, $x = 0.015$, $T = 45$ K. We note two peaks for $\text{Im}(\varepsilon) = \varepsilon_2(\log \omega)$, both symmetric in $\log \omega$. Associated with these peaks are two steps of $\text{Re}(\varepsilon) = \varepsilon_1(\log \omega)$, related by the Kramers–Kronig equation (Lines and Glass 1977). Thus, half of these data are redundant and we restrict ourselves to an analysis of $\varepsilon_2(\log \omega)$. Since presentation of all data sets would require 70 figures, we parametrise our data at the outset.

If ε_2 is a symmetric function of $\log \omega$, as is the case for each of the well separable peaks in figure 3, then one may express the susceptibility in terms of either Debye's equation

$$\varepsilon_2(\omega) = \Delta\varepsilon\omega\tau/(1 + \omega^2\tau^2) = \tfrac{1}{2}\Delta\varepsilon[\cosh(\ln \omega\tau)]^{-1} \tag{1}$$

which is symmetric in $\ln \tau$, or its generalisation

$$\varepsilon_2(\omega) = \Delta\varepsilon \int \mathrm{d}\tau'\, g(\tau')\omega\tau'/(1 + \omega^2\tau'^2) \tag{2}$$

where $\Delta\varepsilon$ is the ε_1 dispersion step amplitude.

Since the distribution $g(\tau')$ must be symmetric in $\ln \tau'$, we may choose a Gaussian

$$g(\tau') = \pi^{-1}\Delta \ln \tau \exp[-(\ln \tau' - \ln \tau)^2/(\Delta \ln \tau)^2]$$

centred at $\ln \tau$ and with a width $\Delta(\ln \tau)$. There are, in general, three parameters to be determined; one of them, $\Delta(\ln \tau)$, may vanish, thus providing the link between equation (2) and its special case, equation (1).

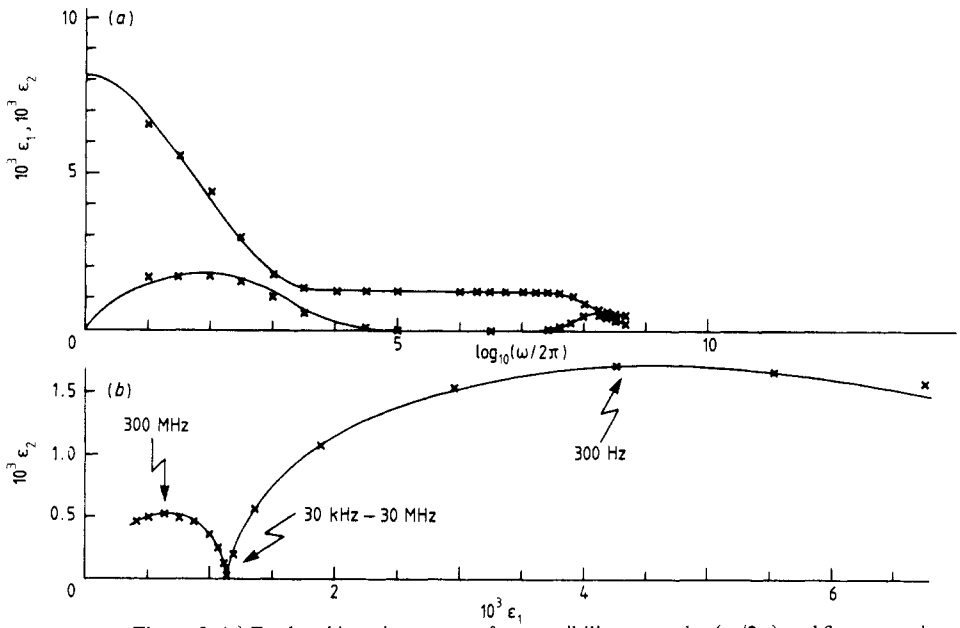

Figure 3. (*a*) Real and imaginay parts of susceptibility versus $\log(\omega/2\pi)$ and fit to equations (1) and (2) of text. Sample is $K_{0.985}Li_{0.015}TaO_3$, $T = 45$ K. (*b*) Real versus imaginary part of susceptibility (Cole–Cole plot) for same data. Note that the high-frequency mode is described by a semicircle centred at the abscissa corresponding to the Debye expression. The low-frequency mode is described by a flat curve with $\varepsilon_{2\max}/\Delta\varepsilon < \frac{1}{2}$. The flattening is a measure for the width of the distribution of relaxation times.

These equations are based on a physical model: a single particle jumps between two wells with a most probable rate of τ which has a standard deviation since the barrier between two wells is also distributed. We shall use this formula derived from the distribution of activation energies as a mere mathematical tool to describe data in closed form (Macdonald 1987), until we have gained more physical insight.

In figure 3, there are two different dispersion regimes: one at high frequencies (HF) and one at low frequencies (LF). Parametrising the data in figure 3 with equation (2) yields two sets of fitting parameters: $\Delta\varepsilon_{\rm hf} = 1140 \pm 100$, $(\tau_{\rm hf})^{-1} = 6 \times 10^8\,{\rm s}^{-1}$, $\Delta(\ln \tau_{\rm hf}) = 0.2 \pm 0.2$; and $\Delta\varepsilon_{\rm lf} = 7 \times 10^3$, $(\tau_{\rm lf})^{-1} = 6 \times 10^3\,{\rm s}^{-1}$, $\Delta(\ln \tau_{\rm lf}) = 3 \pm 0.3$.

The values of the parameters depend only insignificantly on the choice of the distribution, whether Gaussian, Lorentzian or even rectangular. These and the following data were parametrised with the help of equation (2) and a Gaussian distribution $g(\tau)$. A full curve fits the data satisfactorily and at the same time determines $\varepsilon_\infty = 100 \pm 100$. Some readers may be more familiar with plots of ε_2 versus ε_1 such as shown in figures 3(*b*). The fit of the data (to the left) to a perfect semicircle centred at the abscissa indicates that for these high-frequency data equation (2) is obeyed, while the curve drawn through the data, approximately a semicircle centred *below* the abscissa, indicates that for the low-frequency data this is not true. Plots of ε_2 versus ε_1 are suited for quick reference but are a poor analytical tool since all explicit information on frequency is lacking (figure 3(*b*)).

We follow these relaxation peaks in different samples through different temperatures. We have evaluated the size of the peaks $\Delta\varepsilon = (2/\pi) \int {\rm d} \log \omega\, \varepsilon_2(\omega)$ at high

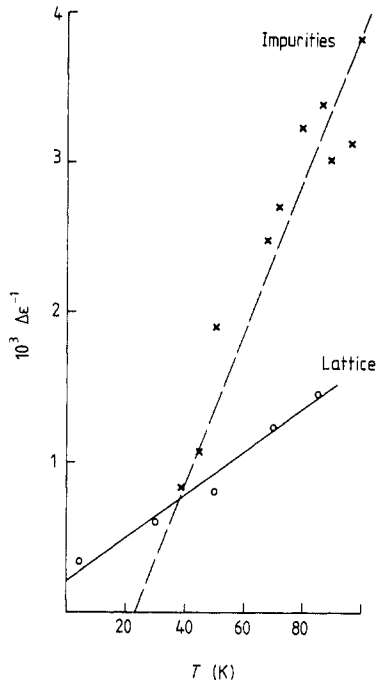

Figure 4. Dielectric dispersion steps $\Delta\varepsilon^{-1}$ of monodispersive high-frequency (○) and polydispersive low-frequency (×) relaxation step. Fits to $C^{-1}(T - T_i)$ and $C^{-1}(T - T_i)$ give $T_i = -15$ K and $T_i = 22$ K for the condensation of lattice and impurity modes, respectively. Sample is $K_{0.994}Li_{0.006}TaO_3$.

(○) and low frequency (×) and plotted the inverse in figure 4. Both $\Delta\varepsilon_{hf}^{-1}(T)$ and $\Delta\varepsilon_{lf}^{-1}(T)$ allow fits to linear functions of T. In standard dielectric jargon, this is equivalent to fits to a Curie–Weiss law $\varepsilon^{-1} = C^{-1}(T - T^C)$. Curie points T^C are given as $T_{lf}^C = 22 \pm 8$ K and $T_{hf}^C = -17 \pm 5$ K and the Curie constant as $C_{lf} = (2.0 \pm 0.3) \times 10^4$ K and $C_{hf} = (7.2 \pm 0.7) \times 10^4$ K. We anticipate the identification of the relaxation peaks as due to the lattice (high frequency) and to the impurity system (low frequency).

In figure 5, we have plotted position and width of both peaks in a somewhat unusual $\ln \tau^{-1}$ versus T diagram. For this purpose we have chosen the sample with $x = 0.015$ since its peaks have comparable intensities. Figure 5 serves to illustrate that the high-frequency peak is monodispersive throughout and that the low-frequency peak is polydispersive with its width increasing upon approaching T_{lf}^C. We note that the modes are mostly well separated and each retains its character where they superimpose (near 100 K). The dispersion steps of this sample are given in figure 6. For high frequency (○), we find $T_{hf}^C = -34$ K and $C_{hf} = 7 \times 10^4$ K; for low frequency (●), $T_{lf}^C = 43$ K and $C_{lf} = 2.5 \times 10^4$ K. In the same figure, we report the relaxation rate τ_{hf} (×), which also follows a Curie–Weiss law with $T_{hf}(\tau^{-1} = 0) = -40$ K. Analogous findings for the high-frequency relaxation step are summarised in figure 7. It shows for $x = 0.026$, 0.04 and 0.06 that $\Delta\varepsilon^{-1}$ decreases with T, leading to large negative effective Curie points which we have not attempted to evaluate quantitatively. For the concentration $x = 0.026$, we present the results of two samples of different shapes and evaluate a scatter of the order of 5%. The low-frequency properties of these samples have been published earlier (Van der Klink *et al* 1983, Höchli 1982).

Some distribution widths for the low-frequency dispersion are shown on logarithmic scale versus T in figure 8. The parameters in the figure indicate the concentration x. Note that $\Delta(\ln \tau) = 2.3$ means a spread of the relaxation-time distribution by an order of

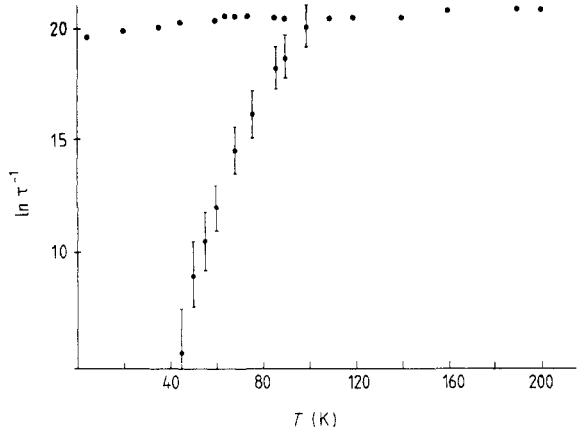

Figure 5. Lattice relaxation time represented by dots (near 20 on ln scale) and impurity relaxation distribution, strongly temperature-dependent. Note that the error bars indicate the Gaussian width of that distribution, not the experimental error. Sample is $K_{0.985}Li_{0.015}TaO_3$.

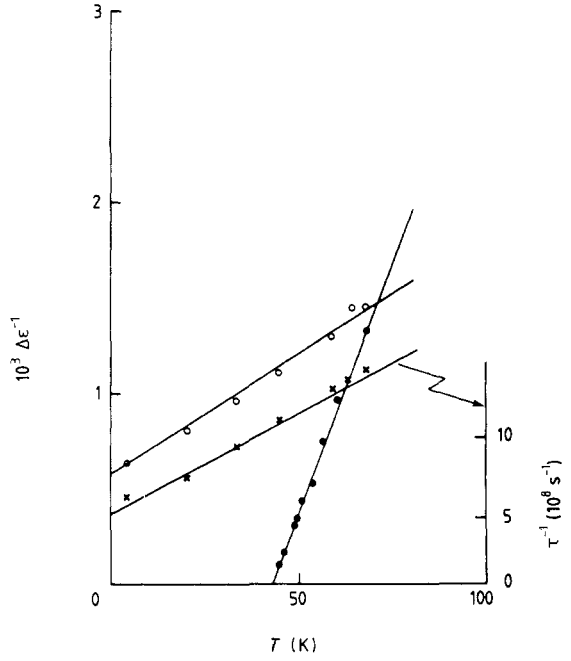

Figure 6. Dielectric dispersion steps $\Delta\varepsilon^{-1}$ in $K_{0.985}Li_{0.015}TaO_3$. The size of the monodispersive step (○) fits to $\Delta\varepsilon^{-1} = -1C(T - T_{hf}^{C})$ with $T_{hf} = -35$ K. The size of the polydispersive step (●) fits to $\Delta\varepsilon^{-1} = C_{lf}^{-1}(T - T_{lf}^{C})$, $T_{lf} = +45$ K. Also shown is the lattice relaxation rate τ_{hf}^{-1} (×) fitting $T - T_{hf}^{C}$, with $T_{hf}^{C} = -40$ K.

magnitude in each direction. For all x except 0.06, $\Delta(\ln \tau)$ increases on approaching T_c and for increasing x. For $x = 0.06$ (figure 8) and other samples with $x > 0.04$ (Van der Klink *et al* 1983, Smolensky *et al* 1986), there are two distinct low-frequency relaxation

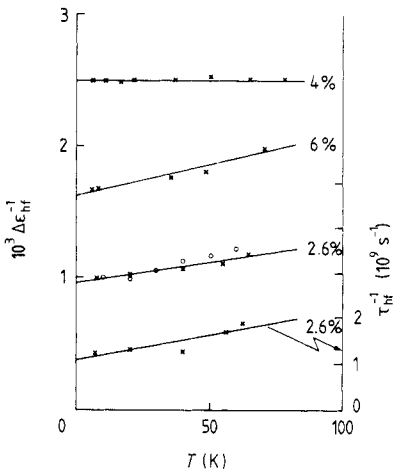

Figure 7. High-frequency dielectric dispersion steps $\Delta\varepsilon^{-1}$ of $K_{1-x}Li_xTaO_3$ versus temperature for $x = 0.026$, 0.04 and 0.06. Straight lines intercept abscissa at $T_{hF}^{C} = -200$ K, $\sim -\infty$ and ~ -200 K for the respective concentrations x. Also shown is τ_{hf}^{-1} for $x = 0.026$, fitting $T - T_{hf}$ with $T_{hf} = -100$ K.

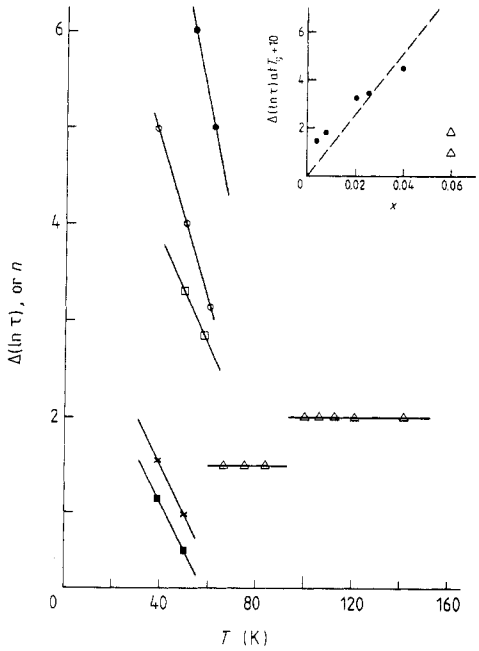

Figure 8. Width of relaxation distribution $\Delta(\ln\tau)$ or, equivalently, density of metastable states versus temperature and for different Li concentrations: (■) 0.004, (×) 0.008, (□) 0.020, (○) 0.026, (●) 0.04, (△) 0.06. Note drastic change of behaviour between $x = 0.04$ and 0.06.

peaks in addition to the HF peak. We evaluate their widths as $\Delta \ln\tau = 2$ and 1.5 independent of T. In the insert, we plot $\Delta \ln\tau$ at $T = T_g + 10$ K versus x and find a monotonic increase up to $x = 0.04$. The sample with $x = 0.06$ clearly has exceptional behaviour.

In certain regions in the T–x diagram, the susceptibilities depend on temperature cycling. We have designated such a region in figure 9 where we plot ε_1 versus T with frequency as a parameter. Except for the addition of new data at high frequency, this plot is almost identical to the one that served to stress the analogy in $K_{1-x}Li_xTaO_3$ with a spin glass (Binder and Young 1986, see figure 3).

Upon temperature cycling, an apparent hysteresis is found for $x = 0.026$ in the range boxed in figure 9. We have enlarged this box in the insert of figure 10 where we show the apparent hysteresis effect. In addition, we report data of ε_1 versus time after cool-down in the same range and note that the sample reaches equilibrium in about 10^4 s. The apparent hysteresis effect is larger in a more concentrated sample, $K_{0.96}Li_{0.04}TaO_3$ (figure 10). Here again, what appears to be hysteresis is in fact slow relaxation.

We summarise the experimental results thus: The dielectric susceptibility in lightly doped $K_{1-x}Li_xTaO_3$, $x \leqslant 0.04$, has two dispersion steps, one monodispersive at high frequency ($\sim 10^8$ Hz) and one polydispersive at temperature-dependent frequencies between 10 and 10^8 Hz. This high-frequency dispersion step does not diverge (in size) nor slow down at any temperature $T \geqslant 0$, whereas the low-frequency dispersion peak

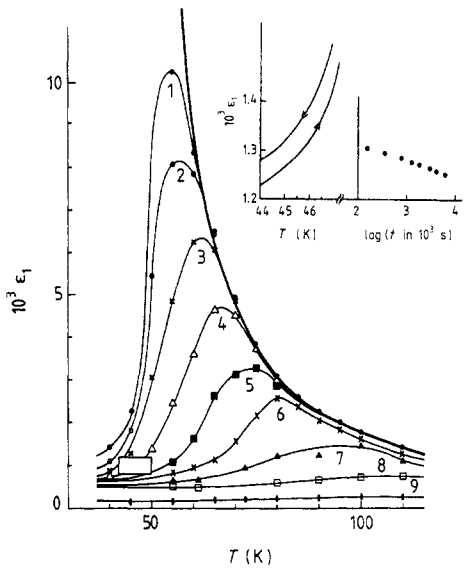

Figure 9. Real part of dielectric susceptibility as a function of temperature, with $\log_{10}$(frequency) as parameter. Sample $K_{0.974}Li_{0.026}TaO_3$. Same growth as Kleemann *et al* (1987). Boxed area: region where Kleemann *et al* observed hysteresis effects. The thick full curve is a fit to Curié–Weiss law. $C = 9 \times 10^4$, $T_c = 50$ K. Inset shows hysteresis effect within the small boxed area and time effect on ε_1 at $T = 45.3$ K.

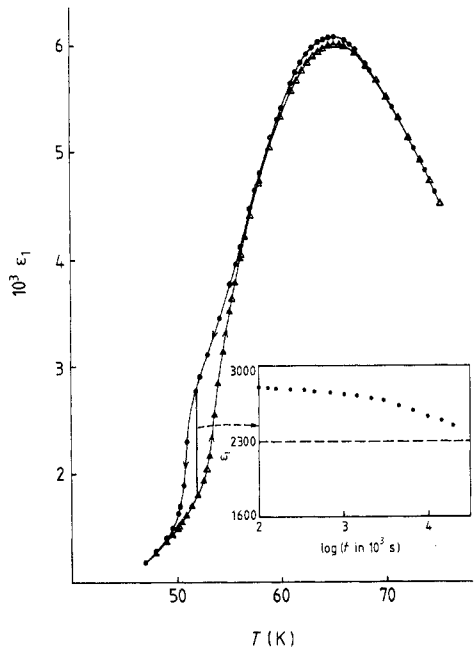

Figure 10. Temperature hysteresis of ε_1 (1 kHz) in $K_{0.960}Li_{0.040}TaO_3$ upon cycling of the sample temperature. Inset: time dependence of ε_1 at $T = 52$ K, largest after hysteretic cycling.

extrapolates to ∞ at the Curie temperature T^C. In heavily doped $KTaO_3$, $x > 0.04$, the lowest-frequency step has characteristics identical to the one above and, in addition, there is a second broadened step besides the usual lattice step.

In the following, we concentrate on the less complex low-concentration regime. We look for models which explain the criticality of the static response of the impurity in Curie–Weiss terms and its unusual broad features, keeping in mind that the high-frequency lattice polarisability does not diverge in the range of the critical impurity response.

We shall also take into account recent data on dielectric relaxation by Smolensky *et al* (1986), on birefringence by Kleemann *et al* (1987) and on neutron scattering by Kamikatahara *et al* (1987), all taken on $KTaO_3$:Li. Each of these groups tended to consider their own set of data as evidence in favour of one specific model, and this resulted in contradictory statements. Thus we attempt here to review all models quoted and to confront them with as much experimental evidence as possible.

3. Theoretical models

A microscopic theory must take into account the presence of local dipoles p_i. They may be either sources of mutual interaction or local fields acting on a regular lattice.

3.1. Random-interaction models (the 'spin-glass' models)

These models imply a Hamiltonian

$$\mathcal{H} = -\sum_{ij} J_{ij} p_i p_j - \sum_i E p_i \tag{3}$$

in which the interaction J_{ij} is random and E independent of i. In this model, the polarisability of the lattice is accounted for by *effective* interactions; in particular, the interaction between magnetic dipoles in conducting hosts, called spin glasses, is represented by a term J_{ij} whose sign oscillates with distance between site i and j (Binder and Young 1986). In analogy, effective interactions between electric dipoles, as simulated by Wang (1980), display the effects of the polarisable lattice. As proposed by Edwards and Anderson (1975), these interactions may be expressed in terms of average $\bar{J}$ and variance $\mathrm{Var}(J)$.

The most explicit results for precursor dynamics come from Monte Carlo simulations on models taking nearest-neighbour interactions $+J$ and $-J$ distributed randomly. They predict that the leading relaxation time goes as $\tau \sim \exp(-E_b/kT)$ (Binder and Young 1986). Below T_c, responses are too slow to be tested by the Monte Carlo method. Instead, a self-consistent mean-field treatment of the Langevin equation (Sompolinski and Zippelius 1981)

$$\frac{\partial p_i}{\partial t} = \frac{1}{kT\tau_0}\frac{\partial \mathcal{H}}{\partial p_i} + \eta_i(t) \tag{4}$$

yielded the result that the susceptibility went as $\varepsilon_2 \sim \omega^{\nu}$, $0 < \nu(T) < \frac{1}{2}$. Here $\mathcal{H}$ is the Hamiltonian of equation (3), η_i Gaussian noise and τ_0 a timescale factor (Binder and Young 1986). This result implies that the leading relaxation time is replaced by a broad distribution peaking at ∞.

Broadening of relaxation times does not occur abruptly at T_g. The Arrhenius-type relaxation above T_g suggests that dipole reorientation occurs over a barrier which does not change critically with temperature. Barriers are, however, subject to local fields whose distributions were calculated by Fisher and Klein (1976) on the basis of random dipolar interactions. They report broadening of the field distribution as $(T - T_c)^{-1}$ and the onset of a polar order parameter $\langle \bar{p} \rangle$ at T_c. The notion of a hierarchy of metastable states prompted Palmer *et al* (1984) to construct a model of hierarchical relaxations. The response function to a Heaviside-type electric field $E = E_0$ for $-\infty < \tau < 0$ is a stretched exponential

$$\Phi(\tau) \sim \exp[-(t/\tau)^n]. \tag{5}$$

This function describes many experimental findings not only in spin glasses but also in other systems. Its Fourier transforms are broadened relaxation peaks much like those obtained by convolution of the Debye response with a distribution of activation energies.

Within random-interaction theory, the interacting species appear to show a response which is broadened with respect to the Debye response. Upon approaching T_g, broadening increases and the leading relaxation rate decreases (at least) as $\exp(-\Delta/kT)$. Below T_c, the effective distribution of relaxation times peaks at ∞ (Sompolinski and Zippelius 1981). These findings were derived on the basis of dynamical models assuming a vanishing mean value of J_{ij}. Its variance can be expressed in terms of a distribution of probabilities for J_{ij}, and this serves for analytical work. The choice of $J_{ij} = \pm 1$ randomly at nearest sites serves for computer simulation.

Interestingly enough, the qualitative behaviour of these two models is not too dissimilar (Binder and Young 1986).

The question of non-zero mean value of J_{ij} has been addressed by Vugmeister and Glinchuk (1980). They assume that a dipole at site r_k couples to a polar lattice mode and that dipoles at site r_e feel the reaction field of the polar lattice mode. They show that this indirect interaction is particularly strong for lattice modes associated with ferroelectric near-instability of the host. It is thus restricted to distances between dipoles of the order of coherence length ξ of the host lattice. They find that this effective interaction has a ferroelectric component of order

$$J \sim \exp(-r/\xi) \tag{6}$$

and conclude that near the instability of the lattice, i.e. for large ξ, the interaction between dipoles is of ferroelectric nature.

However, when they apply their result to $KTaO_3$:Li, they overlook that the reaction field of the polar modes at the Li site (the Lorentz field) vanishes (Slater 1950), as in fact it does for any centrosymmetric site. Accordingly, in the bilinear coupling scheme they applied, there is no interaction between Li and small-k polar-lattice motion. Furthermore, their limiting form of dipolar interaction at large distances as given by Vugmeister and Glinchuk (1980) is at variance with the dipolar form by a factor of $\gamma/(\varepsilon_0 - \varepsilon_\infty)$ even for sites with non-zero Lorentz factor γ. At displaced Li positions, the Lorentz field does not vanish for each single site; it has, however, random character and vanishes for the average of all dipolar occupancies. The assumption of a translation-invariant Lorentz field γ *presupposes* that the Li are ferroelectrically aligned, rather than proving it. Vugmeister's results (Vugmeister and Glinchuk 1980, Vugmeister 1985) are in quantitative error and inapplicable to centrosymmetric sites; their conclusions as to the nature of the $KTaO_3$:Li ground state cannot be maintained. There is, however, no doubt that a polarisable lattice modifies the interaction of dipoles also at centrosymmetric sites. The question of non-zero T_g, while $\bar{J}_{ij}$ vanishes, has been addressed by Carmesin (1988). He finds that a glass phase may be stabilised by cubic anisotropy, which is amply evidenced in $KTaO_3$:Li (Van der Klink *et al* 1983).

Wang (1980) has numerically simulated effective dipolar interaction in an NaCl lattice. He finds strong fluctuations of the effective interaction in size and direction from one site distance to the next. At distances exceeding some 10 Å, interaction becomes truly dipolar with the proper screening factor ε^{-1}. However, even at very short distances there is no sign for the onset of a ferroelectric component. This investigation suggests that the variance rather than the average interaction is enhanced by lattice polarisability.

3.2. Random-field models

The Hamiltonian

$$\mathcal{H} = -\sum_{ij} J_{ij} p_i p_j - e_i p_i \tag{7}$$

is of the random-field type if e_i is a local field with variance. The interaction J_{ij} has translational symmetry and the order parameter is p_i. In the absence of e_i, it has a true ferroelectric (or otherwise ordered) ground state. The random field introduces spatial disorder but it preserves replica symmetry and thus the trivial double degeneracy of

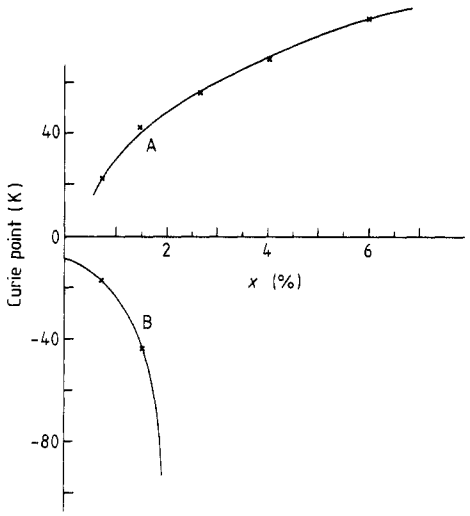

Figure 11. Curie points for the impurity system (curve A) and the host lattice (cruve B). Not shown are the values for $x = 0.026$, $T^{C}_{\text{lattice}} \simeq -200$ K, and $x = 0.04$, $T^{C}_{\text{lattice}} \simeq -\infty$.

the ground state (Schneider and Pytte 1977). The conceptual simplicity of the random-field model has allowed investigations on critical dimensionality and on the stability of domain configurations. We focus on work cited by Kleemann *et al* (1987) as pertinent to the ground state of $K_{1-x}Li_xTaO_3$. Harris (1976) showed that random fields due to impurities shifted a transition in proportion to their concentration and that the correlation length (and hence the susceptibility) remained finite at T_c. His argument was extended to first-order transitions by Imry and Wortis (1979), who suggested that an (unspecified) variable lost its discontinuity when impurities were added. Random fields may thus break up the otherwise homogeneous polarisation into domains. The model of competition between random (impurity-site) fields and ordering (lattice-site) fields presupposes the existence of ferroelectricity in the absence of impurities.

4. Interpretations

In this section, we shall identify the two relaxation peaks denoted by 'high frequency' and 'low frequency' in the experimental section. The properties of these modes will be tested against theoretical predictions in an attempt to select models free of inconsistencies. Dielectric and other data from the literature for this system are also included in our consideration.

4.1. Identification of relaxation peaks

First we analyse the monodispersive high-frequency peak in terms of the expression found, for example, in Lines and Glass (1977).

We recall that, according to the Debye model,

$$\varepsilon^*(T, x, \omega) - \varepsilon(T, x, \infty) = \Delta\varepsilon(T, x)/[1 + j\omega\tau(T, x)] \tag{8}$$

and that the relaxation strength is given by

$$\Delta\varepsilon(T, x) = C(x)[T - T^{C}(x)]^{-1}. \tag{9}$$

We denoted T^C as the Curie temperature of the lattice and show in figure 11 that it is

negative and decreases with x. The Curie constant $C(x)$ is within 20% independent of x and equal to that of pure $KTaO_3$. The characteristic relaxation time behaves as $\tau^{-1}(T, x) = \tau_0(x)[T - T_0(x)]/T_0(x)$; T_0 is negative for all x and τ_0 has the same order of magnitude for all x, including 0.

Thus, these findings describe a monodispersive mode which is also present in pure $KTaO_3$ and suffers only quantitative modifications upon Li doping. It is a relaxational lattice mode whose frequency stays finite (minimum 72 MHz) for all $x \leqslant 0.06$ and all temperatures. Accordingly, in zero field, the lattice has *no long-wave static polar distortion* under any condition. On the contrary, the decrease of the Curie point to large negative values on increasing x shows that Li actually *stabilises the $KTaO_3$ lattice against ferroelectricity*. These findings are in contrast to results in $K_{1-x}Na_xTaO_3$ and $KTa_{1-x}Nb_xO_3$ reported earlier (Maglione *et al* 1987).

We proceed by analysing the polydispersive low-frequency mode in terms of the dispersion step

$$\varepsilon^*(T, x, \omega) - \varepsilon(T, x, \infty) = \Delta\varepsilon(T, x) f(\omega). \tag{10}$$

Two entirely different approaches allow the determination of $f(\omega)$ which both fit the data. The first implies that the dipoles are able to hop over barriers at a rate of $\tau^{-1} = \nu_0 \exp(-\Delta/kT)$. In view of randomness of the systems, the barrier heights are distributed. For a Gaussian distribution, we have (Macdonald 1987, Höchli 1982)

$$f(\omega) = \pi^{-1}\Delta \ln \tau \int \mathrm{d}(\ln \tau') \exp\{-[\ln(\tau'/\tau)/\Delta \ln \tau]^2 (1 - \mathrm{j}\omega\tau)^{-1}\}. \tag{11}$$

The second approach implies that relaxation takes place through a series of metastable states. If τ is the leading relaxation time and n an index related to the density of relaxation times on log scale as $n/(1-n)$, then series relaxation leads to a dielectric dispersion

$$\varepsilon^*(\omega) = \int \mathrm{d}t \exp[\mathrm{i}\omega t - (t/\tau)^n] \tag{12}$$

which is the Fourier transform of the stretched exponential (Palmer *et al* 1984), known also as the Kohlrausch or Williams–Watts function (see Jonscher 1983). In the experimentally accessible range, $\varepsilon_2/\varepsilon_{\max} \geqslant 0.02$, the two expressions (11) and (12) fit the data and can be fitted by one another. On the basis of a dispersion curve alone, it is thus impossible to distinguish between parallel and series relaxation (Macdonald and Hurt 1986)†.

The temperature dependence of the leading relaxation time provides us with circumstantial evidence. Above T_g, it is given by an Arrhenius function, suggesting that the concept of dipoles crossing barriers is valid. Near T_g, τ varies faster than with Arrhenius, indicating the onset of relaxation through a series of metastable states. According to this scenario, the crossover from (mainly) parallel to (mainly) series relaxation takes place at T_g.

The polydispersive mode has

$$\Delta\varepsilon^{-1} = C^{-1}(T - T_g) \tag{13}$$

with T_g increasing monotonically with x. Furthermore, the relaxation times of these

† These authors have drawn attention to the ambiguity between series and parallel relaxation on the basis of a numerical analysis.

modes correspond to those found for the ^{7}Li nucleus in magnetic resonance data (Van der Klink *et al* 1983). Identification of the polydispersive mode as impurity mode is thus straightforward.

Interestingly, the freeze-out of the impurity mode at T_g leaves the lattice mode unaffected: there is no discontinuity of ω_l at T_g. Furthermore, there is no evidence of mode coupling occurring where the two modes are in resonance condition (at 100 K, figure 5). The lattice mode consisting of $k \simeq 0$ displacements of Ta against their oxygen cage is apparently orthogonal on Li reorientations by 90° which involve complex oxygen motion as well. This orthogonality reflects the fact that the reaction field of the lattice modes at the Li site vanishes by symmetry (Slater 1950).

At concentrations higher than $x = 0.04$, there are two distinct impurity modes (Höchli and Baeriswyl 1984) (plus the usual lattice mode), with relaxation rates decreasing like Arrhenius functions with temperature. Their dispersive widths, plotted in figure 8 for $x = 0.06$, are non-zero and temperature-independent. Susceptibility data have also been presented by Smolensky *et al* (1986) for $x = 0.1$ and $x = 0.15$. They draw semicircles through their data in ε_2 versus ε_1 representations, implying Debye relaxation. The fits are, however, not convincing: both above and below T_g, their ε_2 decreases monotonically with frequency from 0.1 to 3×10^3 Hz. Rather, these results indicate that relaxation peaks below the reported frequency range and that the relaxation distribution is broad. Accordingly, for $0.06 \leqslant x \leqslant 0.15$, the transition is from para-electric to a polar state containing disorder. Does this state also contain non-zero polarisation in the sense of Toulouse's (1980) mixed state?

Static non-zero impurity polarisation implies that a $k = 0$ impurity mode must freeze out, implying a slowing down of a monodispersive mode at the transition temperature T_{lf}^C and with the intensity proportional to x. For this there is no evidence, and accordingly the static $k = 0$ polarisation, if present, must be small with respect to local polarisations (which are of the order of the field-cooled polarisation).

The ground state of high-concentration $K_{1-x}Li_xTaO_3$ is different from that at low concentration. While we do not identify it with Toulouse's 'ferroelectric' state, we cannot exclude that it is a 'mixed' state with non-trivial degeneracy (or metastability) and non-zero polarisation. For a positive identification, evidence for non-zero polarisation should as yet be provided.

On the basis of apparently hysteretic susceptibilities, Kleemann *et al* (1987) proposed that (for $x \geqslant 0.26$) $K_{1-x}Li_xTaO_3$ underwent a first-order ferroelectric transition. Our data showed that in the hysteresis region the sample is, in fact, not in equilibrium. We presented evidence for metastability by a direct measurement of the time-dependent susceptibility at $T =$ constant and find time constants compatible with those associated with the breakdown of ergodicity for the same sample (Höchli *et al* 1985). In addition to the inadequacy of the hysteretic polarisation measurement by Kleemann *et al* (1987), the theoretical models they quote, namely by Imry and Wortis (1979) and Imry and Ma (1975), are inapplicable to $KTaO_3$. In these models, the interaction between lattice constituents causes the ground state (Harris 1976) to be ferroelectric whether the transition is first- or second-order. If the impurities are identified as sources of random fields, as in Kleemann *et al* (1987), then the pure lattice must be ferroelectric. This is contrary to all experimental evidence (Landolt-Börnstein 1981). Their attempt to construct a model in which single Li ions act as fields and other Li ions as lattice constituents inducing ferroelectricity suffers from three shortcomings:

(i) The division of Li impurities according to their role in the lattice is arbitrary.

(ii) The clustered Li ions should move faster than the supposedly static fields produced by single ions. This is in contrast to the findings of Binder and Young (1986) that $\tau \simeq \exp(\alpha N)$, where α is of the order of 1 and N the cluster size.

(iii) The lattice mode in $KTaO_3$:Li does not freeze, as required in the model by Imry and Wortis (1979).

4.2. Data other than dielectric

Dipolar relaxation is associated with magnetic relaxation of the ^{7}Li nucleus. NMR probes the local properties of the electric field generated by the Li dipole and acting on the nuclear quadrupole of ^{7}Li with nuclear spin $\frac{3}{2}$. The main results of a recent NMR investigation are the identification of Li as the source of disorder and the discovery that the polar phase is reached by gradual freezing of Li motion (Van der Klink and Borsa 1984).

Lattice relaxation is associated with inelastic scattering of light and neutrons. Both experiments confirm the hardening of the lowest lattice mode at $T = 0$ with growing Li concentration (Prater *et al* 1981a, b, Kamikatahara *et al* 1987). This confirms that Li stabilises the lattice against conventional ferroelectricity. In addition, Prater *et al*'s (1981a) broad Raman response implies the existence of disorder in zero-field-cooled samples, and the observation of time-dependent scattering of neutrons by Kamikatahara *et al* (1987) provides evidence for metastability. X-ray scattering has revealed no structure change to within $c/a - 1 \simeq 3 \times 10^{-5}$ for $x = 0.026$ and a polar coherence of 100 to 1000 Å below T_g (Andrews 1985). Since Li ions have an almost negligible reflection coefficient for x-rays, these coherence lengths quoted by Andrews (1985) refer to polar displacements of Ta. The fact that they remain finite and that the evolving low-temperature configuration depends on time is evidence against ferroelectricity.

Birefringence is a valuable tool to inspect single crystals and may be used for quantitative analysis whenever regions of homogeneous polarisation are large compared to $\lambda \simeq 0.5\ \mu$m. Prater *et al* (1981a) have therefore restricted their quantitative analysis to homogeneous field-cooled samples. Kleemann *et al* (1987) attempt to separate the contributions of cluster susceptibility from those of wall susceptibility on the basis of birefringence data. The evaluation of their data requires knowledge of light propagation in media that are inhomogeneous in the 100 Å scale (Andrews 1985) and averaging over sample sizes of micrometer size. Since the linear superposition of responses they use is inadequate (Bergmann 1978), their conclusions cannot be quantitative.

We have thus reviewed investigations probing local properties (Van der Klink and Borsa 1984), lattice susceptibility via inelastic scattering by light (Prater *et al* 1981a, b, Kamikatahara *et al* 1987), and neutrons and structural coherence (Andrews 1985). The picture emerging from these investigations is one of a host lattice with impurities whose polar motion slows down rapidly and establishes polar disorder. The host lattice is affected only quantitatively by the incorporation of Li, it is made slightly less polarisable and its coherence at $T = 0$ is reduced.

5. Conclusions

Li ions replacing K in the $KTaO_3$ host lattice form local (impurity) dipoles. According to their dynamics, we distinguish two concentration regimes.

At $x \leqslant 0.04$, upon lowering T, dipolar motion becomes exponentially slower in $1/T$ and the dispersive width increases with x and on approaching T_g. In this range, dipole motion is associated to hopping over barriers whose height is distributed owing to the presence of random interactions between dipoles. Near T_g, their motion slows down faster than exponentially in $1/T$. This slow-down is associated to hierarchical relaxation through a series of metastable states which in the time domain has a stretched exponential form.

However, numerical fits of the data alone cannot distinguish between parallel relaxation through a distribution of barriers (equation (11)) and hierarchical relaxation (equation (12)). The proposed distinction between these two relaxation mechanisms rests on the temperature dependence of the response. Below T_g, the dipolar system remains blocked in one of these metastable states which has no net polarisation. Such findings are usually designed in terms of condensation of a glassy phase. Li doping not only introduces local disorder, it also distorts the host lattice in such a way that it becomes stabilised against ferroelectric distortion; the Curie point of the lattice modes decreases monotonically to large negative values as the Li concentration grows from 0 to 0.04.

For concentrations $x \leqslant 0.06$, there are two distinct relaxation phenomena whose distribution width is temperature-independent and clearly non-zero. The ground state for highly concentrated $K_{1-x}Li_xTaO_3$ is thus disordered as for low x, but the disorder effects for $x = 0.06$ are smaller than those for $x = 0.04$ and apparently of static nature. There is no evidence for freeze-out of a net ($k = 0$) polarisation. While these findings exclude the trivial disorder of ferroelectric domain configuration, they do not allow identification with a glass state either. The data for $x \geqslant 0.06$ might be explained in terms of non-random occupation of Li defects in the lattice.

The description of the ground state rests on the observation of the precursor 'order' phenomena. As for ordered systems, spectroscopy of precursor dynamics provides a wealth of information on disordered impurities and the ordered lattice simultaneously. The information, however, pertains to an effective ground state for experimental purposes which is in fact a sampling of metastable states whose lifetime is large compared with seconds. This state does correspond to the states observed by other experimental methods, making comparisons meaningful. Ultimately, allowing for charge compensation by electronic carriers during days, this ground state may be further modified, such as is found for the domain structure of conventional ferroelectrics.

Acknowledgments

We have benefitted from most stimulating discussions with D Baeriswyl and J R Macdonald.

References

Andrews S R 1985 *J. Phys. C: Solid State Phys.* **18** 1357
Bergmann D J 1978 *Phys. Rep.* **43** 377
Binder K and Young A P 1986 *Rev. Mod. Phys.* **58** 801
Carmesin H O 1988 *Z. Phys.* accepted for publication
Edwards S F and Anderson P W 1975 *J. Phys. F: Met. Phys.* **5** 965

Fisher B and Klein M W 1976 *Phys. Rev. Lett.* **37** 756
Harris A B 1976 *J. Physique* **67** 1671
Höchli U T 1982 *Phys. Rev. Lett.* **48** 1494
Höchli U T and Baeriswyl D 1984 *J. Phys. C: Solid State Phys.* **17** 311
Höchli U T, Kofel P and Maglione M 1985 *Phys. Rev.* B **32** 4546
Imry Y and Ma S K 1975 *Phys. Rev. Lett.* **35** 543
Imry Y and Wortis M 1979 *Phys. Rev.* B **19** 3580
Jonscher A K 1983 *Dielectric Relaxation in Solids* (London: Chelsea Dielectrics)
Kamikatahara W A, Loong C K, Ostrowski G E and Boatner L A 1987 *Phys. Rev.* B **35** 223
Kleemann W, Kütz S and Rytz D 1987 *Europhys. Lett.* **4** 239
Landolt–Börnstein, New Series 1981 Group III, vol 16a ed. K-H Hellwege and A M Hellwege (Berlin: Springer)
Lines M E and Glass A M 1977 *Principles and Application of Ferroelectrics and Related Materials* (Oxford: Clarendon) p 999
Macdonald J R 1987 *J. Appl. Phys.* **61** 700
Macdonald J R and Hurt R L 1986 *J. Chem. Phys.* **84** 496
Maglione M 1987 *Thesis* Ecole Polytechnique Fédérale de Lausanne
Maglione M, Rod S and Höchli U T 1987 *Europhys. Lett.* **4** 631
Palmer R G, Stein D L, Abrahams E and Anderson P W 1984 *Phys. Rev. Lett.* **53** 958
Prater R L, Chase L L and Boatner L A 1981a *Solid State Commun.* **40** 697
—— 1981b *Phys. Rev.* B **23** 5904
Rytz D 1984 *Thesis* Ecole Polytechnique Fédérale de Lausanne
Schneider T and Pytte E 1977 *Phys. Rev.* B **15** 1519
Slater J C 1950 *Phys. Rev.* **78** 748
Smolensky G A, Nadolinskaya E G, Yskin N K and Skilnikov A V 1986 *Ferroelectrics* **69** 275
Sompolinski H and Zippelius A 1981 *Phys. Rev. Lett.* **47** 359
Toulouse G 1980 *J. Physique Lett.* **41** 447
Vand der Klink J J and Borsa F 1984 *Phys. Rev.* B **30** 52
Vand der Klink J J, Rytz D, Borsa F and Höchli U T 1983 *Phys. Rev.* B **27** 89
Vugmeister B E 1985 *Sov. Phys.–Solid State* **27** 716
Vugmeister B E and Glinchuk M D 1980 *Sov. Phys.–JETP* **52** 482; *Sov. Phys.–Solid State* **21** 735
Wang J C 1980 *Phys. Rev.* B **22** 2725